

## **Radar Based System for Space Situational Awareness**

**Dipl.-Ing. Jan Eilers**

**Simon Anger MSc.**

**Dr.-Ing. Thomas Neff**

*German Aerospace Center, Oberpfaffenhofen, Germany*

### **Abstract**

Very often existing space situational awareness (SSA) networks include sensors originally not designed for the purpose of space situational awareness. In addition different kinds of sensors are used which makes it even more complicated to fuse all generated data. Creating a network consisting of sensors with a homogenous data interface is therefore a reasonable objective. Technologies available for detection and tracking of objects (e.g. electro-optical sensors or radar) will be discussed with a focal point on operational availability and reliability. It will be shown that especially regarding this aspects radar systems are the most reasonable technology to be used creating a sensor network consisting of interoperable sensors. Nevertheless, electro-optical sensors are important to generate complementary information. The DLR SMARTnet [1] generates this information in a passive way for geostationary satellites and the DLR orbital debris laser ranging station in Stuttgart [2] achieved this task in an active approach, but this paper presents a proposal for a network of radars configured for this purpose. The system is intended to detect and track objects that are at least as small as objects that can currently be found in the United States Space Surveillance Network (US SSN) catalogue [3] but also has the possibility to make high-resolution images of tracked objects. Furthermore potential hazards in different orbits will be evaluated and discussed in order to optimize the system in that direction. The system is supposed to be able to create an own object catalogue. Therefore repeated tracking and required capacity will also be considered.

Technical criteria for detection and tracking of objects will be determined. This part of the work contains aspects like choosing adequate frequency bands for tracking and imaging of different sizes of objects. In the next step the locations for the sensors will be determined. Based on considerations about necessary infrastructure it is plausible to locate the radar systems on existing observation sites. Possibilities for imaging radar systems will be presented, which enables the user to get an image of the object to analyse it technically, in addition to the information of size and orbit. By analyzing simulations, feasible approaches for such a Space Situational Awareness Network will be presented.

Keywords: Space Situational Awareness, SAR-Sensor, Sensor Network

### **1. List of Abbreviations**

DBF	Digital Beamforming
dBsm	Decibel square meter
DLR	German Aerospace Center
FoV	Field of View
GEO	Geostationary Earth Orbit
HEO	High Ecliptical Earth Orbit
IoSIS	Imaging of Satellites in Space
ISAR	Inverse Synthetic Aperture Radar
LEO	Low Earth Orbit
MEO	Medium Earth Orbit
PA	Phased Array
PRF	Pulse Repetition Frequency
RCS	Radar Cross Section
SNR	Signal to Noise Ratio
SSA	Space Situational Awareness

T/R	Transmit and Receive
TLE	Two Line Element
US SSN	United States Space Surveillance Network

## 2. Introduction

It is well known, that space situational awareness (SSA) becomes more and more important for the safety of civil and military spacecraft because the number of artificial objects orbiting the Earth steadily increases. The most comprehensive data base comes from the United States Space Surveillance Network (US SSN) which bases on a sensor network consisting of different sensors and sensor types. Keeping in mind the US funding cuts during sequestration that have degraded two line elements (TLEs) quality in late, creating a network consisting of sensors with a homogenous data interface to support the worldwide effort to build up and maintain a data base with high precise TLEs of as many as possible objects orbiting Earth is a reasonable objective.

One aspect of SSA is the knowledge of position, orbits, size and shape of all potential harmful objects. Aside the fact that there are approx. 22.000 elements in the public US SSN catalogue the true number of space objects is much higher and can differ considerably from orbit altitude, shape and material. The size of objects that have to be detected and tracked due to their potential to catastrophic collisions can be obtained by using the NASA Breakup Model [4]. If the energy to mass ratio exceeds 40J/g, a collision might imply a loss of the satellite. As it can be seen in Fig. 1 the risk for potential collisions is highest at an altitude of about 800 km due to the peak in spatial density.

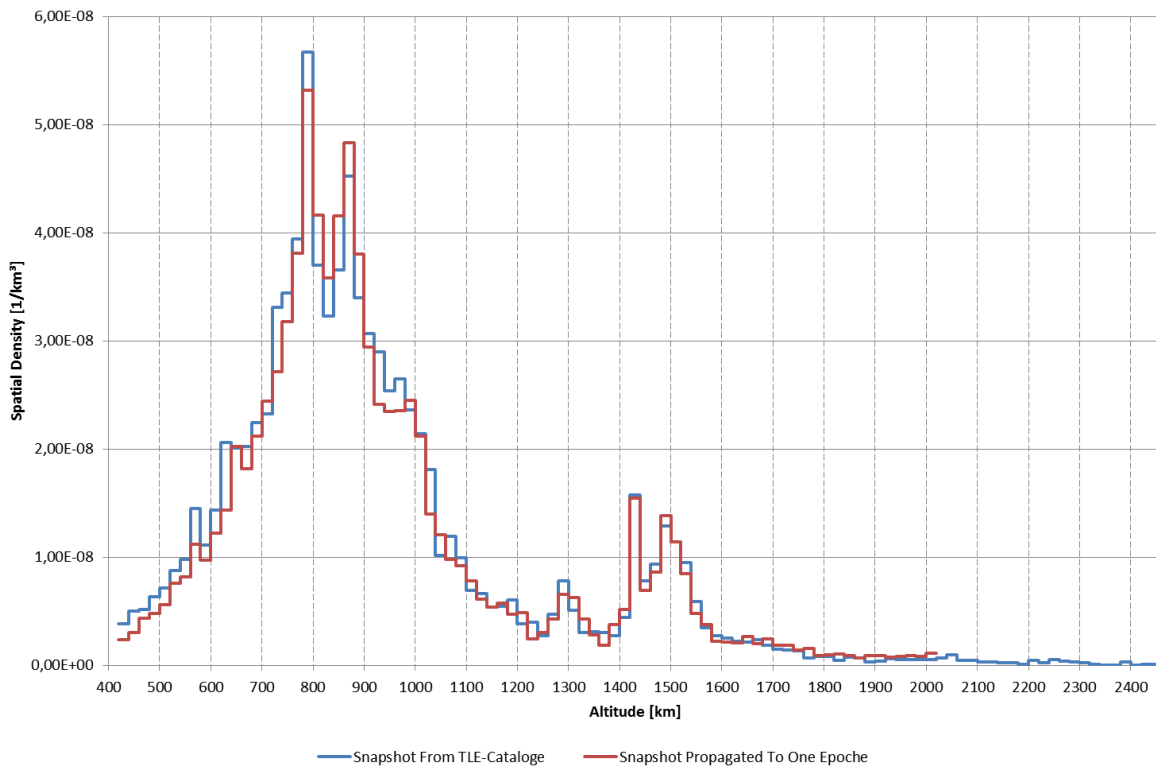


Fig. 1: Spatial density distribution of objects in space based on the US SSN catalogue, represented by a snapshot of given orbital elements and additionally propagated to one specific time instance.

The spatial density is only one measure to characterize a piece of a space situation. Another characterization is illustrated in Fig. 2. This graph shows the number of possible collision partners for each individual object in the US SSN catalogue with the blue line and the orbit classification with a yellow dot as well as the amount of objects for a specific orbit type on the right side. For each object the amount of orbit intersections with other objects has been calculated based on a minimum orbit intersection distance of e.g. 1000 meters for potentially hazardous objects. Those orbits have usually a similar semi-major axis or they possess a high eccentricity. The approximate sum of possible collisions based on information in the US SSN catalogue is about 88.170.000. The analysis of several orbit altitudes over a longer time period can lead to the information how endangered a specific orbit is with respect to collisions.

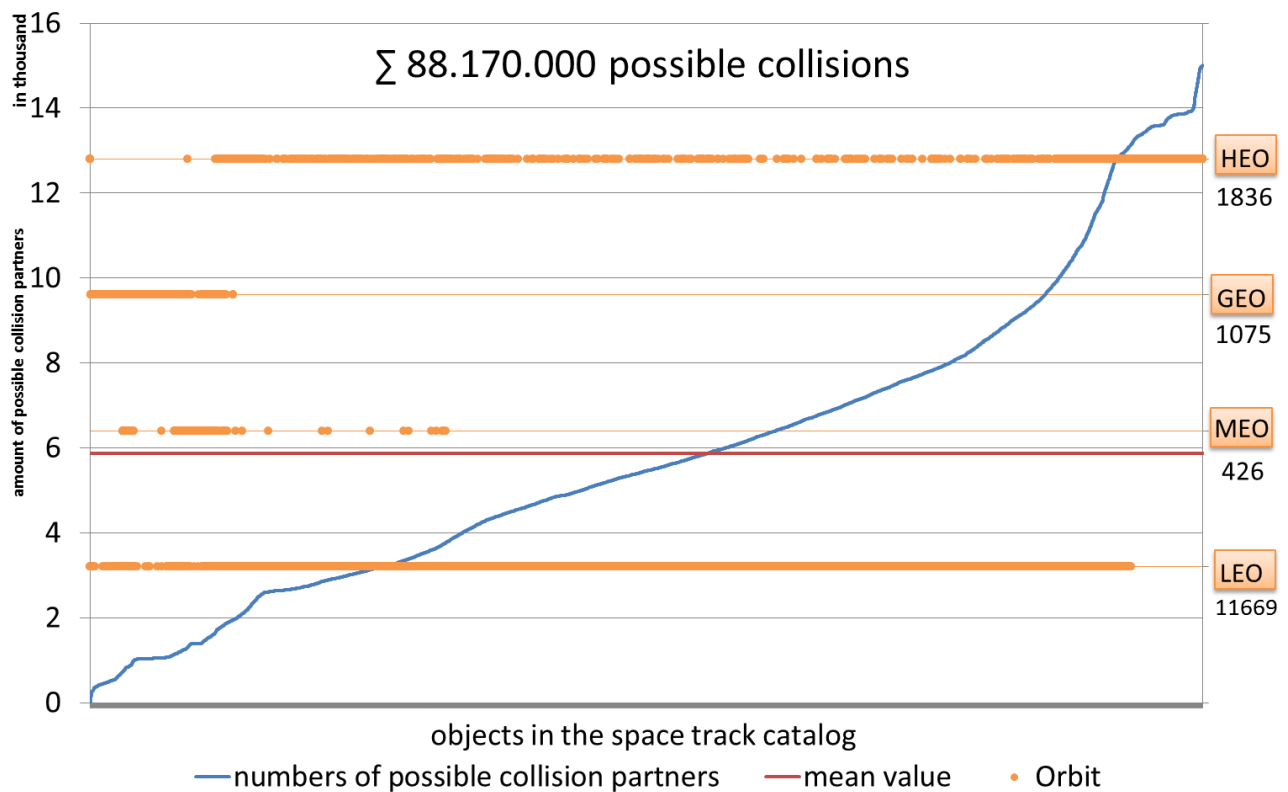


Fig. 2: Computation of possible collision partners in conjunction with the distribution of each individual classification of object orbit (LEO, MEO, HEO, GEO).

However, this question raises another question: “How reliable is the information on which the analysis is performed?”. A closer look at the Two Line Element (TLE) data in the catalogue is illustrated in Fig. 3. This catalogue information was downloaded on 2013-01-24. The oldest TLE epoch is dated on 2012-12-26 and hence it is about 29 days old. 836 TLE sets have an epoch older than 6 days and most of them are located in low earth orbit (LEO). But these objects within the catalogue are only a subset of objects which are located in space and which are defined as trackable. In one night of observation several thousand objects can be detected but only a few of these objects can be correlated to trackable objects. Furthermore the official US SSN catalogue does not represent all trackable objects.

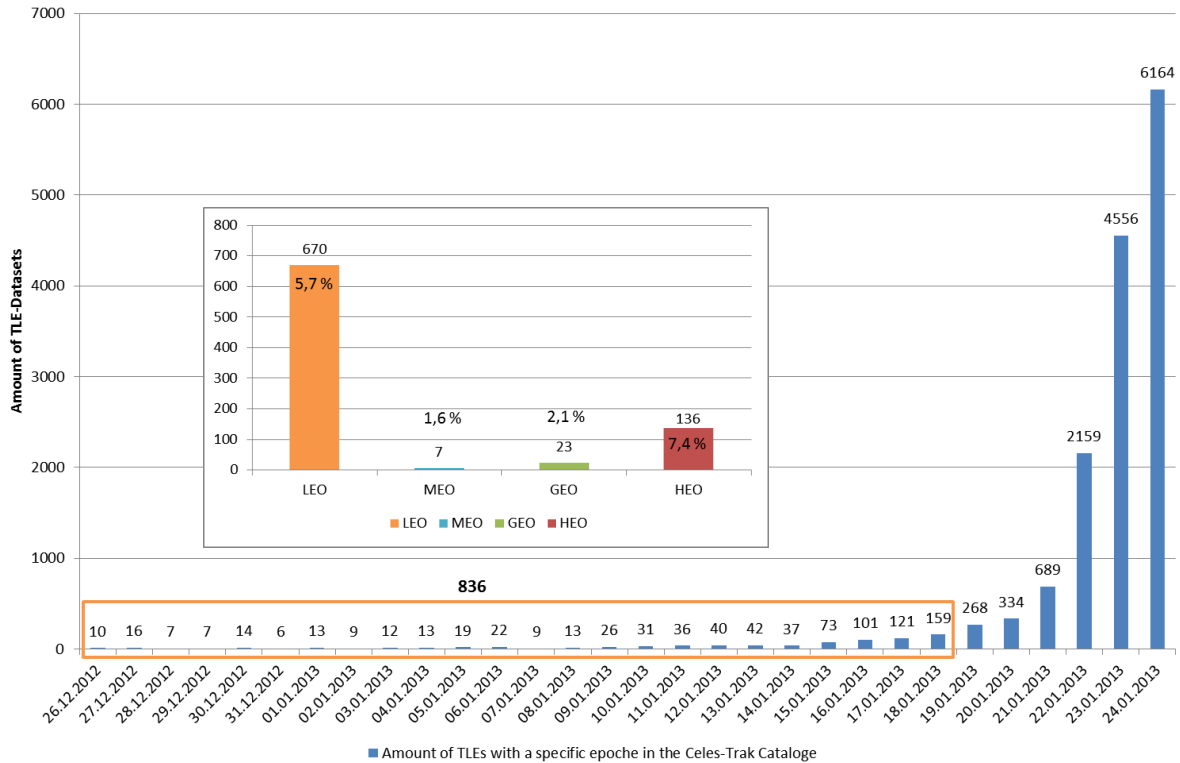


Fig. 3: Distribution of TLE epoch dates within the US SSN catalogue of one day (2013-01-24) and the spread of objects with older TLE epoch dates over different orbit types.

For a holistic space situational awareness (SSA), enabling full protection of our very own space assets, it is necessary to gain information about orbiting objects having different size and different orbit altitudes. Another required input for SSA is the generation of information about the task and/or origin of orbiting objects. These objects can be grouped as detectable, trackable and illustratable depending on the available sensors in the network. The number and the location of the sensors as well as their performance have an impact on the update rate of information about the objects.

The main pillar for comprehensive and reliable SSA is the availability of adequate sensors joined in a network. Different sensor technologies are presently used to observe Earth orbiting objects: optical telescopes and radars, the latter either using mechanical steering or electronic steering by phased array (PA) techniques. Optical telescopes are necessary for higher altitudes (thousands of kilometers) but due to illumination and weather conditions for low earth objects, radar sensors are more successful there. When deciding for phased array radars or mechanically steered ones we have to consider the type of information we want to generate. If state vector and orbit of as many objects as possible is the main task, radars with mechanical steering cannot be used. Conventional phased array radars may also have trouble observing a large amount of objects simultaneously, so therefore nowadays the potential of digital beamforming (DBF) is of major interest. For detailed imaging of orbiting objects and acquiring information about their possible task or origin, a synthetic aperture radar is a suitable sensor.

### 3. Tracking of Objects

#### 3.1 Analyzing field of view and Maximum Range

Before designing radar systems for space surveillance, the desired field of view (FoV) and maximum range of reliable operation have to be evaluated, as they are major design drivers. The desired system here is supposed to be able to detect objects up to an altitude of 2,000 km. Hence the maximum range of the radar required to fully observe this altitude is a function of the minimum elevation angle  $\phi$  of the system. Fig. 4 shows this relationship where  $h$  is the altitude of the objects orbit and  $R_{max}$  the necessary range for observing the object under an elevation angle  $\phi$ .

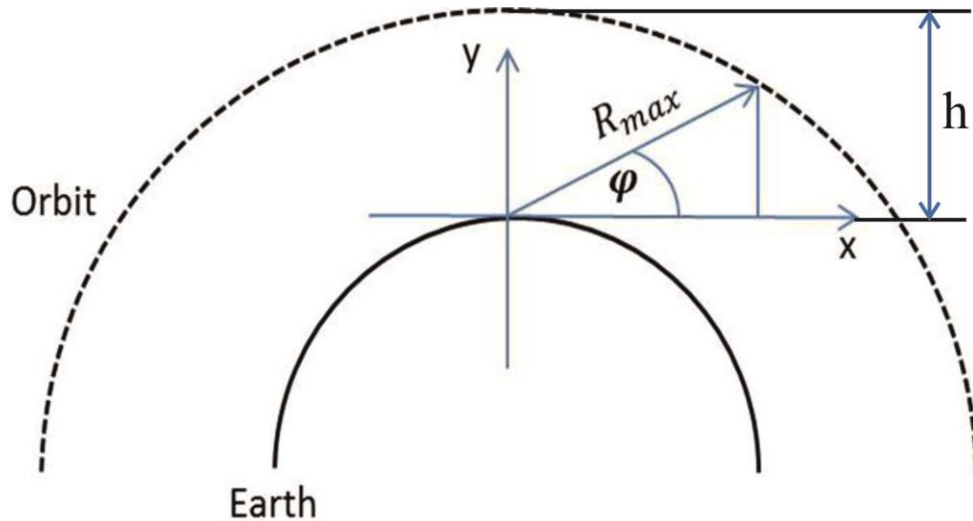


Fig. 4: Determination of required maximum range of a ground-based radar system for space surveillance.

The required range for different elevation angles has been computed. The minimum elevation angle has been assumed to be  $5^\circ$ . So a  $30^\circ$  coverage in elevation leads to maximum elevation of  $35^\circ$ . Now Table 1 shows the required range of the radar sensor for different elevation angles.

Table 1: Required range as a function of elevation angles

Elevation	Required range
$5^\circ$	4,905 km
$15^\circ$	4,027 km
$25^\circ$	3,367 km
$35^\circ$	2,890 km
$45^\circ$	2,549 km
$55^\circ$	2,312 km

It can be recognized that the desired region of elevation angles, together with the maximum orbit altitude, fixes the required operational range of the radar systems, and hence major radar parameters for a desired signal-to-noise ratio (SNR).

In order to analyze the impact of FoV size, the location and observational direction of the radar, simulations for different locations and FoVs have been performed. It can be shown that at least one hemisphere has to be simulated, and the longitude of a sensor position has no impact on the observational performance. All earth orbiting objects were propagated for a period of about 10 days using the USStratCom database. Fig. 5 shows the number of

observable objects for a sensor with a maximum range of 4,000 km at 20° coverage (15° to 35°) in elevation and azimuthal coverage of about 60°, pointing south. As one can see, best locations are in latitudes between 10° and 25°.

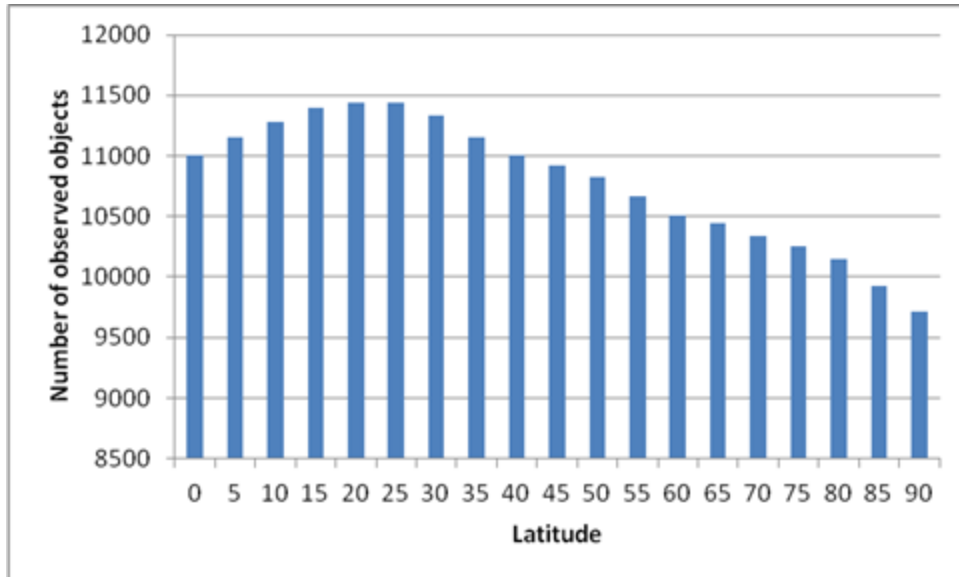


Fig. 5: Observable objects depending on latitude for a radar sensor pointing in south direction, allowing a maximum range of 4000 km, a 20° coverage in elevation angle, and an azimuthal coverage of  $\pm 30^\circ$

An important parameter for the observability of an object is the time span the object is residing within the sensor's FoV. Therefore this parameter can be optimized with respect to other radar parameters. Increasing the azimuthal coverage leads to longer dwell times, increasing coverage in elevation has in the analyzed cases negligible effects on time. As Fig. 6 shows, even 60° azimuthal coverage leads already to considerable dwell times.

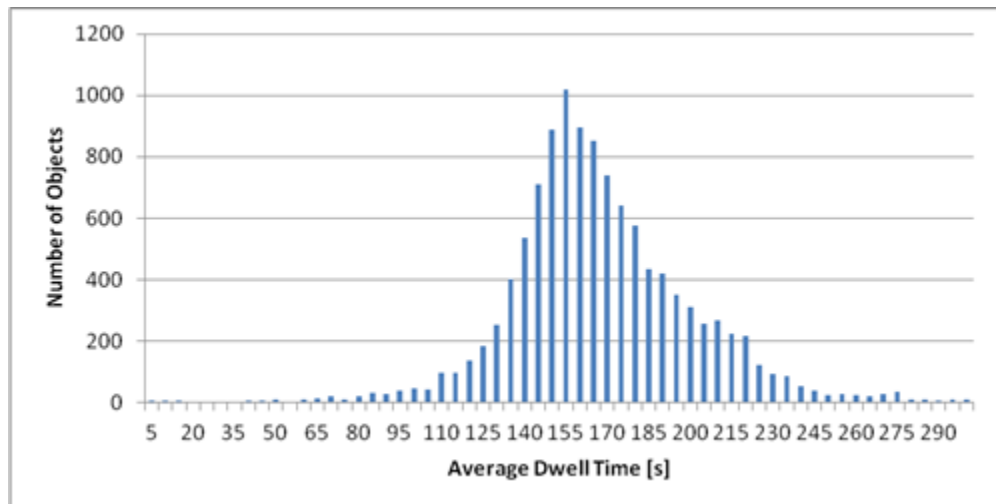


Fig. 6: Average dwell times assuming 2,500 km maximum range of the radar, 60° azimuthal coverage, 20° coverage in elevation angle, assuming 20° latitude of radar position.

Now if digital beamforming is used the dwell times can lead to high integration gain improving SNR, since the object can be observed all the time being in the FoV by a receiving beam. As an example, using a pulse repetition frequency of 47 Hz and an assumed dwell time of 100 s, 37 dB of SNR improvement can be realized. However,

DBF on receive requires a higher amount of transmit power, when the whole FoV shall be illuminated simultaneously.

### 3.2 ANALYZING REQUIRED RADAR PARAMETERS

A further important radar parameter to be set is the waveband or frequency range of the signal. As outlined before it is useful to detect and track objects down to sizes of 5 cm diameter. Based on physical boundary conditions, the radar cross section (RCS) for different wavelengths can differ as shown in Table 2 using as a representative example of a fully metallic sphere of diameter 5 cm.

Table 2: RCS of a fully metallic sphere of diameter 5 cm

Band designator	UHF	X band	W band
Frequency [GHz]	0.43	10	90
Wavelength [m]	0.7	0.03	0.003
RCS [dBsm]	-44.51	-27	-27

The RCS is increasing with decreasing wavelengths till reaching its maximum value of -27 dBsm. This value can already be gained with a wavelength of 0.03 m. In the case of a fully metallic sphere shorter wavelengths do not contribute to better results. Other object shapes and compositions might differ more or less from that tendency.

To ensure that all objects passing the sensor's FoV can be detected, DBF on transmit and receive shall be used. Fig. 7 shows the segmentation of the whole FoV, the beams formed by sub-arrays of the whole antenna array are divided by red lines, the total FoV is bordered in blue.

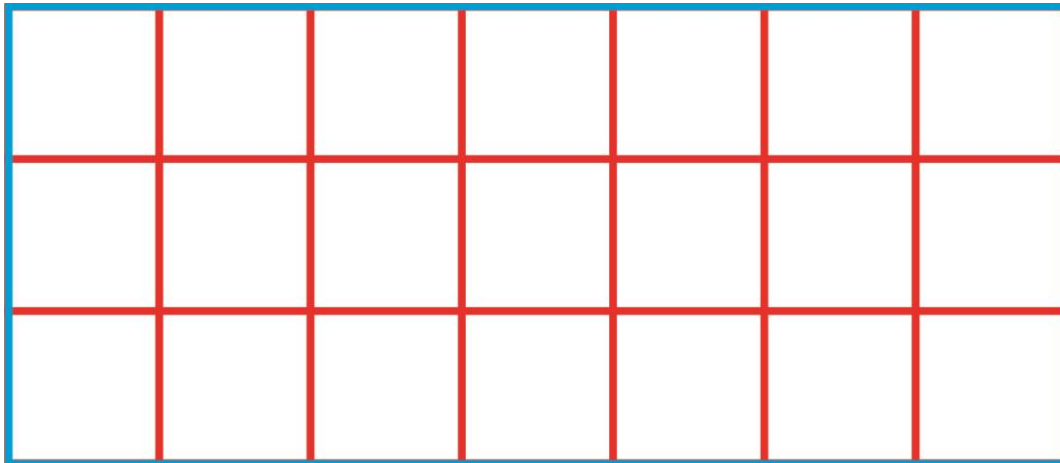


Fig. 7: Segmentation of the FoV by DBF beams.

This concept leads to an increased antenna gain, compared to the one generated for illuminating the total FoV region, since all transmit and receive (T/R) modules can be used for this purpose. The more transmission beams at defined transmit power are used, the better the SNR. However, more transmission beams at fixed transmit power lead to higher total power consumption of the system. Hence a reasonable number and size has to be used as a compromise. It has been found that beam sizes of about 1.5° (3 dB width) lead to satisfying results. Now for instance, when covering 40° in elevation and 60° in azimuth there is a need for at least 1,080 subarrays forming these beams. The system is supposed to create pulsed signals having a duration of 1.3 ms. Using a pulse repetition frequency (PRF) of 47Hz and 50 W maximum peak power of a T/R module, a value which should be available in

near future, this leads to an average power of approximately 3 W per module. Higher PRFs are hard to implement because it takes about 20 ms till the signal returns from a target in a distance of 2,500 km.

### 3.3 Locating Proper Sensor Sites

As shown in section 3.1, the best sensor locations can be found between 10° and 25° latitude. The proposed sensor type requires a lot of infrastructure already available at existing sensor sites. So building up a network using existing sensor sites will be the most efficient plan. In order to evaluate the available locations, all existing SSA sensor sites have been analyzed. Furthermore, using a nearly uniform distribution around the globe minimizes the necessary number of installations. The sites in Hawaii and Tenerife fit the demands very well. A third sensor site then has to be located at longitudes between 110° and 120°. Consequently best infrastructural conditions might be found in Australia but there is no large SSA radar sensor at these longitudes existing yet. Perth has been assumed as a proper location where infrastructural requirements could be fulfilled. Table 3 summarizes the chosen locations for all radar sensors shown in figure 8.

Table 3: Optimized locations for suitable SSA radar sites for full surveillance coverage.

Location	Longitude	Latitude
Tenerife/Spain	-16.51	28.3
Maui/Hawaii/USA	-156.257	20.7085
Perth/Australia	115.63	-31.52

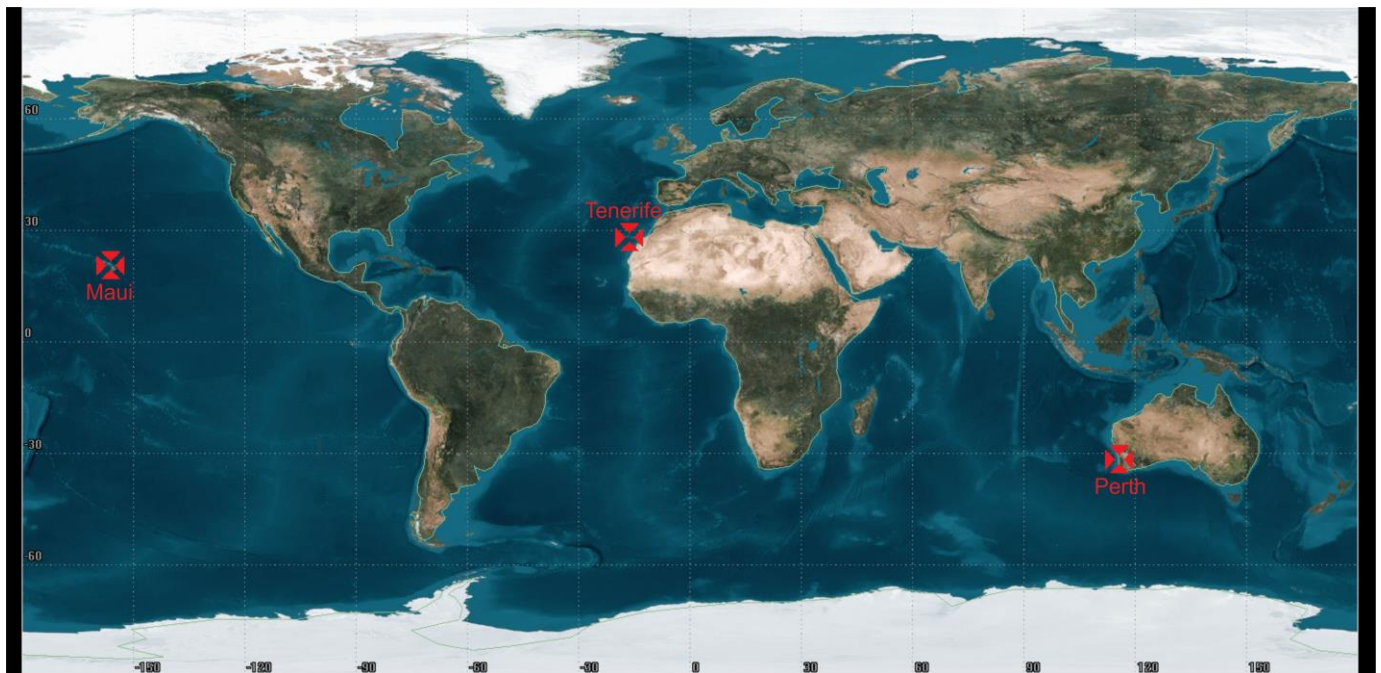


Fig. 8: Proposed sensor locations for full SSA surveillance capability.

These locations and possible combinations have been analyzed. Criteria for a successful correlation of observations from different ground stations for the identical object where set to at least one observation per station every 24 hours with a minimum dwell time of about 10 seconds. The results of the analysis are shown in tables 4 and 5 [4].

Table 4: Correlated percentage of TLE population

Locations	Percentage of population with height of perigee			
	<2,000 km	<1,500 km	<1,000 km	<500 km
Maui-Perth	89.6%	90.1%	89.4%	52.1%
Maui-Tenerife	89.7%	90.2%	89.5%	51.9%
Perth-Tenerife	89.6%	90.1%	89.3%	51.6%
Maui-Perth-Tenerife	90.8%	91.2%	90.6%	58.8%

Table 5: Correlated percentage of TLE population with  $e>0.1$

Locations	Percentage of population with height of perigee			
	<2,000 km	<1,500 km	<1,000 km	<500 km
Maui-Perth	99.7%	99.9%	99.9%	99.8%
Maui-Tenerife	99.6%	99.8%	99.9%	99.8%
Perth-Tenerife	99.6%	99.8%	99.9%	99.7%
Maui-Perth-Tenerife	99.8%	99.9%	99.9%	99.8%

#### 4. Imaging of objects

In order to refine tracking and enabling more detailed analysis of new found objects in addition to the above mentioned DBF radar an additional imaging radar can be used. Imaging radars enable the possibility to get sufficiently high spatial resolution for two-dimensional images of unknown objects based on their spatial distribution of radar cross section. The difference compared to tracking radars is the fact that imaging radars provide more information about the size, shape and possible spin of the object. Thus a radar system for high-performance SSA should consist on one hand of tracking capability to determine the orbit parameters, and on the other hand of the ability to establish high-resolution images. The most suitable imaging principle of inverse synthetic aperture radar (ISAR) is illustrated in Figure 9. Locally fixed ground-based microwave radar and the moving space object at specific orbit together build the requirement for the ISAR imaging geometry. The proper motion of the object generates the required synthetic aperture of length  $L_{SA}$ .  $R_A$  is the range at the beginning and  $R_E$  at the end of the imaging process. A steerable antenna system provides capability of wide azimuth scanning required for high azimuth resolution. In range direction the signal bandwidth determines sufficient range resolution. In parallel the integration time of azimuth observation is extended for very high resolution, resulting in SNR enhancement in the final radar image [5].

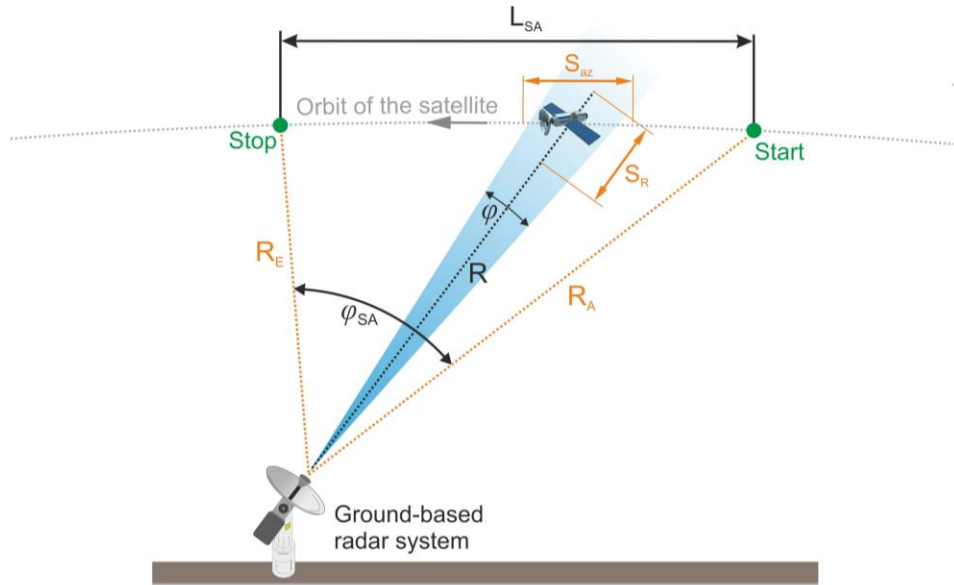


Fig. 9: ISAR geometry for imaging of moving objects in space using a fixed ground-based radar system. The requirements on the radar system for tracking and imaging capability differ in some technical aspects. Considering the imaging radar the basic requirement is high bandwidth in order to get a sufficient range resolution given by:

$$\Delta r = \frac{c}{2B}$$

Here  $c$  is the speed of light and  $B$  the bandwidth of the radar system. Figure 10 shows range resolution as a function of bandwidth. It can be concluded that the bandwidth should be in the order of several GHz in order to get desired range resolution in the centimeter region, being preferable for detecting fine object details.



Fig. 10: Relation between range resolution and bandwidth of the radar system.

In addition, depending on the used center frequency a wide azimuth observation angle is required to achieve similar azimuth resolution given by [7]:

$$\Delta r_{Azimuth} = \frac{c}{4f_c \sin(\varphi_{SA}/2)}$$

Here  $f_c$  is the center frequency and  $\varphi_{SA}$  the observation angle in azimuth direction. Attention should be paid to successful operation of this ISAR approach, which is only valid under the assumption that the RCS of the object is rather constant within the region of azimuth angle  $\varphi_{SA}$ . Figure 12 shows azimuth resolution as a function of azimuth observation angle for different center frequencies. In contrast to range resolution the azimuth resolution depends on center frequency, i.e. as higher the center frequency the lower the required observation angle for constant azimuth resolution. From this perspective a higher center frequency is preferable, but it is very challenging to generate sufficient transmit power at higher frequency ranges, and the higher atmospheric attenuation has also to be taken into account. However, Figure 11 also indicates that UHF band is rather impractical or impossible to achieve azimuth resolution of several centimeters, while X band is a suitable candidate.

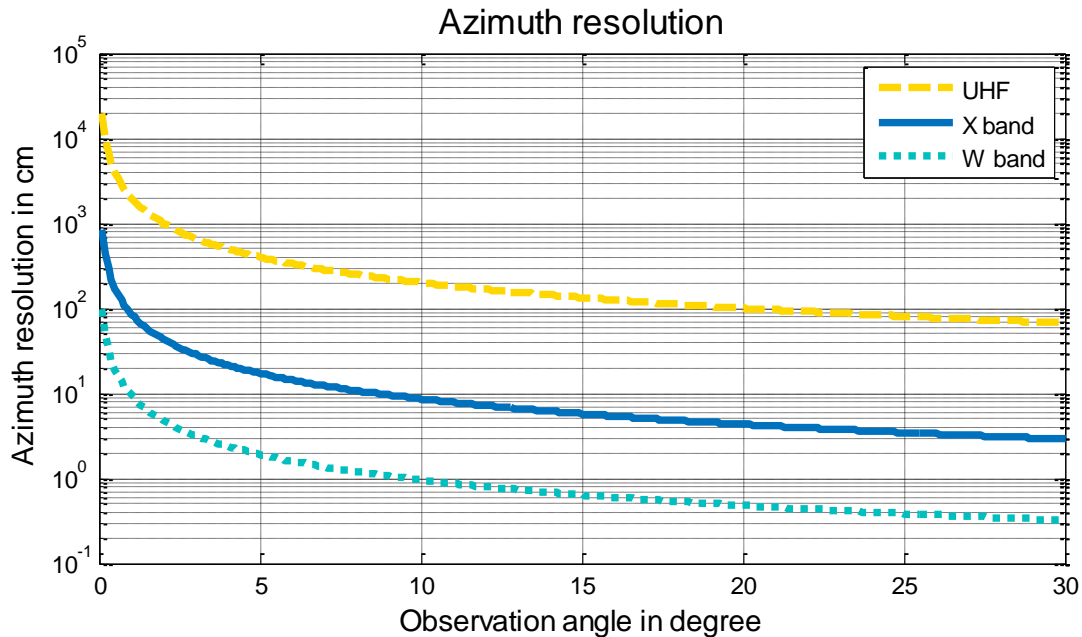


Fig. 11: Relation between the azimuth resolution and observation angle in azimuth direction.

Using ISAR techniques, coherent reception and processing of radar data must be guaranteed in order to form the synthetic aperture. Furthermore, considering imaging radar based on reflector antenna technology and its narrow antenna beam, the orbital parameters of the object to be imaged have to be known in order to control the steerable antenna system. This information could be provided by DBF tracking radar as explained in previous chapters. In addition, several error sources have to be taken into account for such high-performance ISAR imaging, being of no relevance for low-resolution systems. These are, on one hand, internal errors from the radar system itself like the frequency dependent transfer function and the possible jitter of digital components. On the other hand there are external errors from the atmosphere (tropospheric and ionospheric delays), the uncertainty in object position determination and misalignment of the antenna beam.

For the imaging purposes now, an experimental measurement setup (IoSiS – Imaging of Satellites in Space) has been developed by German Aerospace Center (DLR), Department for Reconnaissance and Security, as shown in Figure 12. The technical data of the IoSiS system are given next in Table 6:

Table 6: Important technical parameters of the IoSiS system

Parameter	Value
Wavelength	0.03 m
Peak power	10 kW
Maximum Range	1000 km
Maximum Bandwidth	4.4 GHz
Coverage in Azimuth	150°
Coverage in Elevation	60°
Size of the Rx antenna	1 m
Size of the Tx antenna	9 m

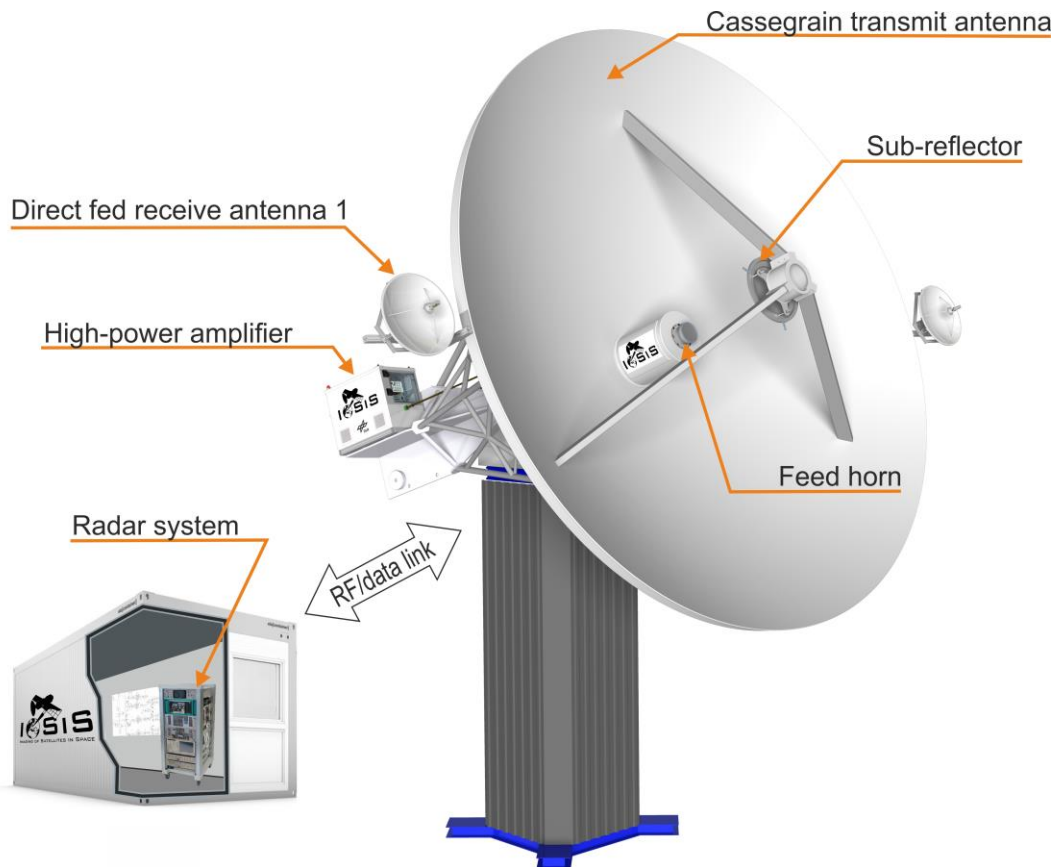


Fig. 12: Hardware setup of the IoSiS system consisting of the GigaRad radar, a high-power amplifier, and a multi-dish based antenna system.

An existing antenna system, normally used as communication link during satellite launches, was adapted to the IoSiS radar system. In a first implementation the experimental measurement setup contains a Cassegrain transmit and two direct fed receive antennas, having a diameter of 9 m and 1 m, respectively. Due to the high gain of the transmit antenna the receive antenna could be constructed much smaller for a desired SNR in the final images. A high-power amplifier is used to generate necessary transmit power required to cover a range of up to 1000 km. The multi-purpose radar system GigaRad, used for high-performance signal generation and reception is located in a container nearby the antenna system [8]. GigaRad is working in a pulsed mode and allows wideband digital signal generation and fast digital signal acquisition of the received pulses in time domain. An RF and a data link are established between the radar and the antenna system. The maximum bandwidth of up to 4.4 GHz allows a range resolution of up to few centimeters. Hence a quadratic resolution cell is achieved using a region for azimuth angle of 24°. This allows high-resolution ISAR imaging of IoSiS already in the experimental phase. During first operations, detailed investigations of the above mentioned error sources can be performed based on real measurement data. A detailed description of the IoSiS measurement setup can be found in [6].

## 5. Conclusion

The problem of increasing objects and space debris in LEOs and the resulting hazard to operational space-borne systems is still challenging and unsolved. The analysis above shows that modern high-performance radar systems can enable the detection, tracking and identification of hazardous earth orbiting objects. The corresponding knowledge of orbital parameters, size, structure and possible origin of objects down to very small RCS values can considerably improve the situation.

## 6. References

- [1] Fiedler, Hauke und Schildknecht, Thomas und Weigel, Martin und Meinel, Michael und Hempel, Rolf und Herzog, Johannes und Prohaska, Marcel und Ploner, Martin (2014) *SMARTnet – First Results of a Test Campaign*. Space Situational Awareness 2014, 03.-04.Nov. 2014, London, Great Britain
- [2] Hampf, Daniel und Riede, Wolfgang und Wagner, Paul und Sproll, Fabian und Humbert, Leif (2015) *Orbital Debris Laser Ranging Station Stuttgart*. ILRS Technical Workshop, 26. - 30. Okt. 2015, Matera, Italien
- [3] [www.stratcom.mil/factsheets/11/Space\\_Control\\_and\\_Space\\_Surveillance/](http://www.stratcom.mil/factsheets/11/Space_Control_and_Space_Surveillance/)
- [4] Johnson N.L., Krisko P.H., Liou J.-C., Anz-Meador P.D., NASA's new breakup model of evolve 4.0, *Advances in Space Research*, Vol 28, Issue 9, pp 1377-1384, 2001
- [5] Liebschwager T., Neff T., Süß H., Förstner R., *Design of a Radar Based Space Situational Awareness System*, Advanced Maui Optical and Space Surveillance Technologies Conference (AMOS), Maui, Hawaii, 2013.
- [6] Anger S., Peichl M., Dill S., Jirousek M., Schreiber E.: *"IoSiS – A high-performance imaging radar for surveillance of objects in low earth orbit"*, Proceedings of European Conference of Synthetic Aperture Radar (EUSAR), Hamburg, Germany, 2016.
- [7] Mensa, Dean L., *High Resolution Radar Cross-Section Imaging*, Artech House, Massachusetts, 1991.
- [8] Anger S., Jirousek M., Peichl M.: *"GigaRad – a versatile high-resolution ground-based pulse radar for advanced remote sensing research"*, Proceedings of European Conference of Synthetic Aperture Radar (EUSAR), Berlin, Germany, 2014.